for the interacting fermion system. In any event, even without the convergence question being settled, the author feels that the present results are at least on a strong a footing as the variational ones. Furthermore, the merit of the present work lies in the method rather than the results for two reasons: (1) It provides a systematic way in which it should be possible to settle the long-range order question by an investigation of the convergence of the perturbation series. (2) The use of linked spin clusters could ultimately lead to a consistent treatment of the collective modes of the antiferromagnetic spin system in a manner similar to Hubbard's[22] treatment of the collective motions of the electron plasma.

ACKNOWLEDGMENT

The author wishes to express his appreciation to Professor Jan Korringa for suggesting the topic of this work; furthermore, the author is indebted to Professor Korringa for his advice and encouragement during the course of the present work.

[22] J. Hubbard, Proc. Roy. Soc. (London) **A240**, 539 (1957).

PHYSICAL REVIEW VOLUME 120, NUMBER 3 NOVEMBER 1, 1960

Dependence of Secondary Electron Emission from MgO Single Crystals on Angle of Incidence

A. B. LAPONSKY AND N. R. WHETTEN
General Electric Research Laboratory, Schenectady, New York

(Received November 24, 1959; revised manuscript received July 21, 1960)

The influence of the angle of incidence of primary electrons on the energy distribution and total yield of secondary electrons from MgO cleaved single crystals has been studied. Charging effects were minimized by using single pulse techniques. The relative number of low-energy secondary electrons decreases with increasing angles of incidence. The effect appears to be most marked at primary energies in the vicinity of the maximum of the yield curve. At lower and higher primary energies the dependence on angle of incidence diminishes. Under most conditions the total yield increases with increasing angles of incidence. The magnitude of the increase is influenced by the primary electron energy. At low energies a slight decrease in total yield with increasing incidence angles has been observed. A dependence of the backscattered fraction of electrons on the angle of incidence of the primaries has been observed at several primary electron energies.

A number of maxima and minima occur superposed on the gross variation of total yield with angle of incidence. The angular positions of the maxima are insensitive to primary energy but show a dependence on the crystal orientation. Several models for accounting for the phenomena are discussed.

I. INTRODUCTION

A NUMBER of workers have investigated features of the dependence of secondary electron yield of solids on the angle of incidence of the primary electrons.[1,2] The yield is generally found to increase as the angle of incidence is increased. Qualitatively this is explained by the decreased distance to the surface that a secondary, produced at a given point along the path of a primary electron, must traverse in order to escape. Except for the work of Shatas, Marshall, and Pomerantz,[2] who have demonstrated that for very high primary energies and thin targets the yield varies according to the relationship $\delta(\theta)=\delta_0 \sec\theta$, quantitative descriptions have been inadequate due to the inability to treat properly both the processes of production and escape of the internal secondary electrons.

The purpose of this paper is to describe several experiments investigating some additional features of the dependence of secondary electron emission on angle of incidence. First the energy distribution of the emerging low-energy secondary electrons is determined as a function of the incidence angle. Secondly the change in total yield with angle of incidence is determined for insulating single crystals of MgO. Finally an unexpected dependence of the secondary electron yield on the direction of the primary electron beam with respect to certain crystallographic directions is described.[3]

II. EXPERIMENTAL PROCEDURE

The MgO single crystal[4] targets employed in this investigation were cleaved along (100) planes to about

[1] H. Bruining, *Physics and Application of Secondary Electron Emission* (Pergamon Press, Ltd., New York, 1954), p. 100. A. J. Dekker, *Solid-State Physics*, edited by F. Seitz and D. Turnbull (Academic Press, Inc., New York, 1958), p. 297.

[2] R. A. Shatas, J. F. Marshall, and M. A. Pomerantz, Phys. Rev. **102**, 682 (1956).

[3] Preliminary accounts of these experiments were presented at the New York and Ithaca meetings of the American Physical Society, 1958 [A. B. Laponsky and N. R. Whetten, Bull. Am. Phys. Soc. **3**, 46 (1958); **4**, 265 (1958)]. Also see A. B. Laponsky and N. R. Whetten, Phys. Rev. Letters **3**, 510 (1959).

[4] The MgO crystals were obtained from Infra Red Development Company, Welwyn Garden City, Hertfordshire, England.

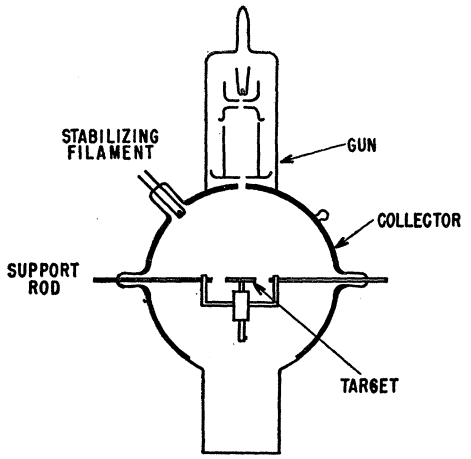

FIG. 1. Experimental secondary emission tube.

1.0 cm square and 0.5 mm thick. All of the measurements were carried out in sealed-off tubes of the type shown in Fig. 1. Each tube consists of an electron gun producing a collimated electron beam of about 3° divergence, a graphite coated secondary electron collector, a stabilizing filament for flooding the crystal with low-energy electrons, and a target holder upon which the crystals could be placed. The target holder was slung from the two rods shown in the figure so that by rotating the tube about the axis of the rods the angle of incidence could be varied. The target holder remained fixed in position under the influence of gravity. In addition to acting as supports the rods served as electrical contacts to the target assembly.

The tubes were processed in two stages. Initially the tubes were evacuated and baked at 400°C and the electron guns degassed by high-frequency heating. Following this treatment the tubes were opened to a dry nitrogen atmosphere and the MgO crystals inserted immediately after cleaving. Subsequent vacuum baking was limited to 250°C. After processing the tubes were sealed off and put into operation under vacua of about 10^{-9} mm Hg or less.

To minimize charging of the crystal surface, measurements utilizing single pulse techniques previously described[5] were employed. The incident charge per pulse could be limited to about 2×10^{-14} coulomb and the change in the target surface potential to about 0.1 volt. Between measurements the target surface potential was reproducibly established by flooding the crystal with low-energy electrons from the stabilizing filament. For this operation the tube was always oriented in the position corresponding to normal incidence.

The measurements required for determining energy distribution and yield curves have for the most part been described previously.[5] The net charge to the target at various collector potentials is measured with the detector in the target circuit. In addition, the primary charge is determined. For positive collector-to-target potentials the measurement in the target circuit gives the total emitted charge in excess of that incident on the target from the primary beam. The use of a −50-volt collector-to-target potential results in a determination of what has often been assumed to be the primary charge. This assumes that the backscattering of electrons from the target can be neglected. Since this assumption may not always be valid, a true measure of the primary charge is obtainable by detecting the pulsed charge in the target and collector circuits combined. These two measurements are related by $q_1=q_t[1-\eta(1-\delta_c)]$ where q_t, q_1, η, and δ_c are, respectively, the true primary charge, the primary charge as detected in the target circuit, the backscattered fraction of the target, and the *effective* secondary emission yield of the collector for the backscattered electrons. The latter is a function of the collector potential. Since δ_c is not known, a measure of the backscattered fraction is not possible although relative changes in η can be determined. Table I gives an estimate of the ratio of the backscattered fraction at 60° to that at 0° for several primary electron energies obtained from measured values of q_1 and q_t. It is apparent that errors in the primary charge as large as 10 to 20% may occur when this measurement is made in the target circuit. For the purposes of this study the primary charge has been taken to be that which is measured in the combined target and collector circuits. By assuming reasonable values for η and δ_c and taking δ_c to be proportional to the target-to-collector potential, the influence of secondaries liberated at the collector on the normalized energy *distribution* curves (Figs. 3, 4, and 5 of the following section) has been found to be negligible.

TABLE I. Ratio of backscattered fraction for 60° and 0° angles of incidence.

Primary energy (ev)	$\frac{q_1}{q_t}$ (0°)	$\frac{q_1}{q_t}$ (60°)	$\frac{\eta\ (60°)}{\eta\ (0°)}$
600	0.89	0.88	1.1
1000	0.91	0.87	1.4
4000	0.90	0.80	2.0

III. RESULTS

The results reported in this section have been obtained from a number of experiments on MgO single crystals. The data are presented as typical of a number of determinations of secondary electron emission dependence on angle of incidence. Energy distribution measurements were made on a total of five different crystals. Seven crystals were employed for the total yield measurements. Unless otherwise specified the results presented here correspond to crystals oriented such that the axis of rotation is a [010] direction while the normal to the crystal surface is a [100] direction.

[5] N. R. Whetten and A. B. Laponsky, Phys. Rev. **107**, 1521 (1957).

A. Secondary Electron Energy Distribution

From measurements of the effective yield at different angles of incidence as a function of collector potential, retarding potential curves were obtained for several primary electron energies. The curves were scaled so that saturation yield corresponded to unity. The retarding potential curves give the relative number of secondary electrons having energies greater than that corresponding to the collector potential (after contact potential corrections). Typical curves obtained at 1000-ev primary electron energy and 60° and 0° angles of incidence over a limited range of collector potentials are shown in Fig. 2. Differentiation of the smoothed retarding potential curves result in energy distribution curves normalized to unit area over the entire energy spectrum of emitted electrons.

Curves of distribution-in-energy of secondary electrons over the low-energy regions of the spectra are

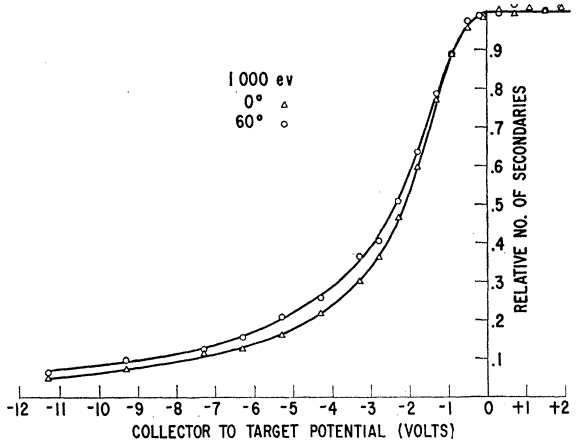

FIG. 2. Retarding potential curves for 0° and 60° angles of incidence of the primary beam. Primary electron energy was 1000 ev. Curves have been corrected for effective contact potential difference between collector and target.

shown in Figs. 3, 4, and 5. These correspond to 600-, 1000-, and 4000-ev primary electron energies, respectively, and are presented for 0° and 60° angles of incidence. The most probable energy of emission, slightly greater than 1 ev, does not depend significantly on the angle of incidence of the primaries within the accuracy that could be expected from numerical differentiations. Curves obtained at 0° incidence angle are relatively richer in low-energy secondaries than those obtained at 60° incidence angle. This dependence is influenced by the primary electron energy. For primary energies near that corresponding to the maximum in the secondary electron yield curve (about 1000 ev)[6] the differences between the secondary electron spectra for the two incidence angles are most pronounced. At lower and higher primary energies the differences between the

[6] N. R. Whetten and A. B. Laponsky, J. Appl. Phys. **28**, 515 (1957).

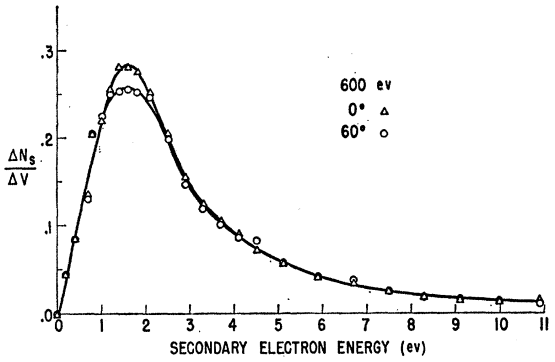

FIG. 3. Curves of distribution-in-energy of low-energy secondary electrons for 0° and 60° angles of incidence of the primary beam. Primary electron energy was 600 ev. Curves have been normalized to unity area over the *entire* spectrum of emitted electrons.

spectra at the two angles diminish. Similar variations have been observed on all the crystals studied and appear, although to a lesser extent, on measurements made at 0° and 45° angles of incidence.

Although some inaccuracies are to be expected from differentiation of the smoothed retarding potential curves, reproducibility of the trends shown in Figs. 3, 4, and 5 on a number of different crystals, and the reproducibility of energy spectra on any given crystal, support the qualitative correctness of the comparisons.

B. Total Yield

Typical measurements of the dependence of secondary electron yield on angle of incidence at primary electron energies of 600, 2000, and 4000 ev are shown in Fig. 6. The yield here is defined as the ratio of the total emitted charge to that incident on the target. The curves are symmetrical about normal incidence for rotation in a given plane. At 600-ev primary energy the yield appears to decrease slightly with increasing angles of incidence. The curves obtained at 2000 and 4000 ev show an increase of yield with angle of incidence. The extent of this increase is dependent on the magnitude of the primary electron energy.

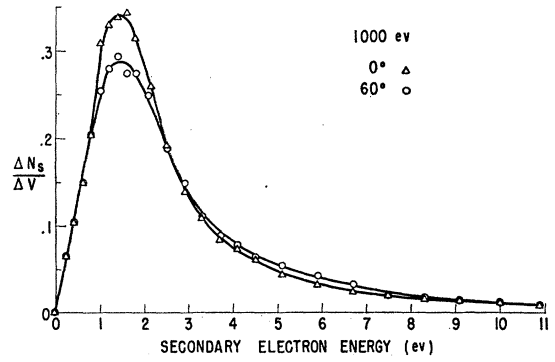

FIG. 4. Curves of distribution-in-energy of low-energy secondary electrons for 0° and 60° angles of incidence of the primary beam Primary electron energy was 1000 ev. Curves have been normalized. to unity area over the *entire* spectrum of emitted electrons.

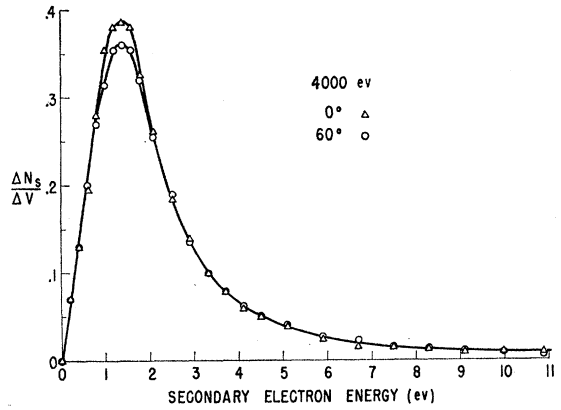

FIG. 5. Curves of distribution-in-energy of low-energy secondary electrons for 0° and 60° angles of incidence of the primary beam. Primary electron energy was 4000 ev. Curves have been normalized to unity area over the *entire* spectrum of emitted electrons.

In addition to the gross dependence of yield on the angle of incidence of the primaries there appear clearly several irregularities in the form of maxima and minima. These have been found consistently on all targets investigated. In the data of Fig. 6 the existence of any such structure at 600-ev primary energy is questionable but is quite clear at 2000 and 4000 ev. The angular positions of the maxima appear at about 43°, 23°, and 0°. The angles have been determined by subtracting from the curves an estimated mean smooth curve of δ vs θ based on the relationship of Bruining.[1] Such a curve is indicated by the dotted curve in the figure. This procedure shows that the maxima which are immediately apparent in the figure may occur at angles slightly different from the true angles of enhancement. With this uncertainty, which may amount to a degree or two depending upon the steepness of the gross curve of δ vs θ, and an inherent broadness in the maxima, the angular positions of the maxima seem to be reproducible to within about 2°. They do not seem to be significantly dependent on the primary electron energy. The sizes of the maxima are, however, influenced by the magnitude of the primary energy.

Figure 7 shows similar curves obtained at 3 and 5 kev on a MgO single crystal oriented so that the axis of rotation was the [101] direction and the normal to the crystal surface, corresponding to 0°, was the [100] direction.

For these curves the maxima occur at about 55°, 44°, 35°, 19°, and 0° for the 3-kev data while for that obtained at 5 kev the maxima at 44° and 19° are missing. A small maximum appears at about 22° in the latter case. These curves again show a dependence of the height of the maxima but not of their angular positions on the primary electron energy.

Comparing the angular positions of the maxima from Figs. 6 and 7, there is seen to be a dependence of these angles on the crystal orientation.

IV. DISCUSSION

A. Secondary Electron Energy Distribution

The energy distribution curves of Figs. 3, 4, and 5 depict the influence of the incidence angle on the low-energy region of the secondary electron spectra. When the diffusion path length for the excited internal electrons to reach the surface is decreased, there occurs a decrease in the low-energy peak height of the spectrum. The diffusion path length also decreases with decreasing primary electron energy. These figures show the previously reported[5] dependence of secondary electron spectra on primary energy for both 0° and 60° angles of incidence.

The differences between spectra obtained at 0° and 60° incidence angles appear to be most marked for data obtained at about 1000-ev primary energy. These differences become smaller at the lower (600 ev) and higher (4000 ev) primary energies. At low primary energies intense scattering of the primary beam near the surface of the crystal reduces the importance of the initial angle of incidence. As the primary electron energy is increased the effect of scattering near the surface becomes less and the secondary electron energy distribution curves at 0° and 60° incidence angles show greater differences. Those at 0° possess a relatively higher low-energy peak and slightly lower tail than those at 60°. This arises due to the decrease in energy degradation of excited electrons in diffusing a shorter distance to the surface for 60° than for 0° angle of incidence.

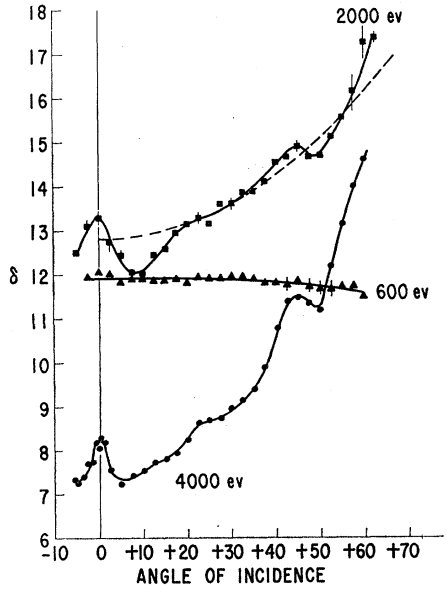

FIG. 6. Dependence of total yield on angle of incidence of 600-, 2000-, and 4000-ev primary electrons. Axis of rotation is a [010] direction while the crystal surface is a (100) plane. Curves are shown for counter-clockwise rotations. Symmetry exists about 0° angle of incidence. The broken curve corresponds to the relation of Bruining, $\delta_\theta = \delta_0 \exp[\alpha x_m(1-\cos\theta)]$ where $\alpha x_m = 2.18$.

In that region of the crystal from which significant numbers of excited electrons can escape as secondaries, further increases in the primary energy result in a further decrease in the scattering of the primary beam. In addition the rate of excitation of electrons in the crystal per unit path length of the primaries tends to become increasingly independent of the depth of penetration of the primary electrons. Under these latter two conditions the number of electrons excited at a given depth, for 60° angle of incidence relative to that at 0°, approaches a value independent of the depth of excitation within the crystal. This results in the normalized secondary electron energy spectra becoming almost independent of the angle of incidence.

B. Total Yield

The total yield decreases slightly with increasing angles of incidence at 600 ev (Fig. 6).[7] At this relatively low energy and correspondingly small penetration depth of the primaries, most of the properly directed low-energy secondaries would be expected to escape from the crystal regardless of the angle of incidence. However,

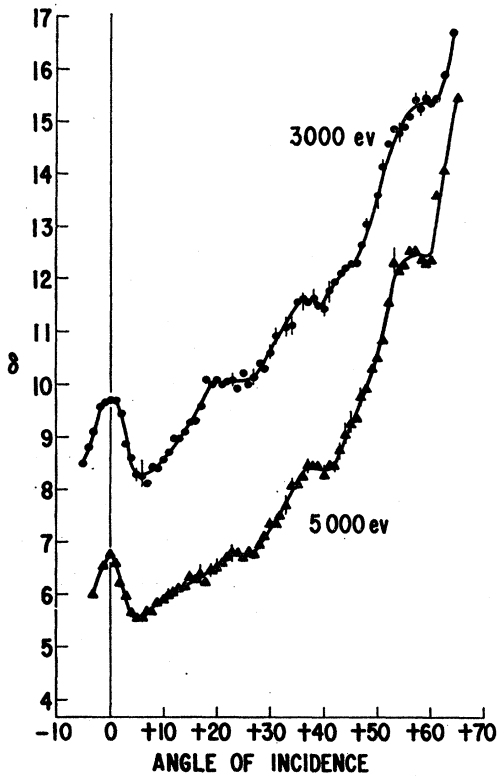

FIG. 7. Dependence of total. yield on angle of incidence of 3000- and 5000-ev primary electrons. Axis of rotation is a [101] direction while the crystal surface is a (100) plane. Curves are for counter clockwise rotations. Symmetry exists about 0° angle of incidence.

[7] A similar decrease at low primary energies has been reported for NaBr and NaF. L. N. Dobretsov and T. L. Matskevich, J. Tech. Phys. U.S.S.R. **27**, 734 (1957) [translation: Soviet Phys. (Tech. Phys.) **2**, 663 (1957)].

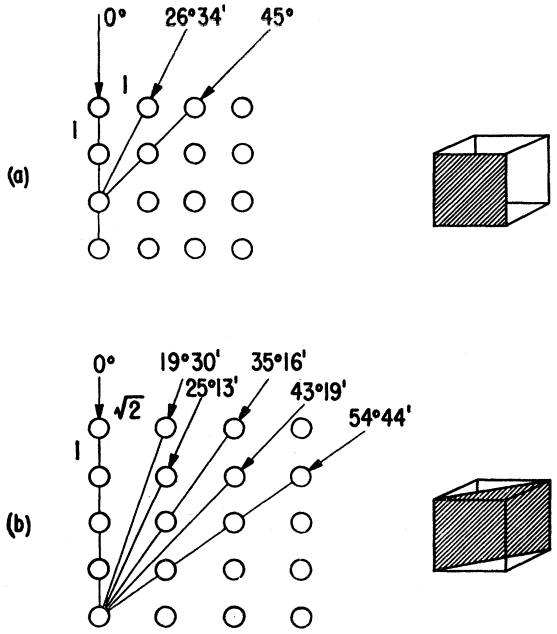

FIG. 8. Atomic arrays for cubic crystal orientations corresponding to Figs. 6 and 7. (a) Rotation about the [010] direction. (b) Rotation about the [101] direction. Shaded areas on the right are normal to the axis of rotation and correspond to the planes for which the atomic arrays are shown at the left.

since increasing the angle of incidence brings the scattering process closer to the surface, greater numbers of the scattered primary electrons and high-energy secondary electrons leave the crystal with sizeable energies. These are consequently lost as secondary-producing electrons. This process manifests itself in the increase in backscattered fraction shown in Table I and the slight decrease in total yield with angle of incidence evident in Fig. 6 for the case of the 600-ev primaries. At higher primary energies the increase in backscattered electrons with increasing angle of incidence is more marked than at 600-ev primary energy. However, at these energies many internal secondaries are produced sufficiently deep within the crystal that significant numbers are unable to escape.[8] Under these conditions an increase in angle of incidence increases the escape probability of the low-energy internal secondaries by decreasing their diffusion path to the surface and results in increasing values of total yield as shown in Figs. 6 and 7.

The dependence of the angular positions of the maxima on the crystal orientations used in the experiments suggests a correlation between low-index crystalline directions and the direction of the primary beam. Figures 8(a) and (b) show schematically various low-

[8] With increasing primary energy at normal incidence the yield increases approximately proportional to the increase in primary energy to roughly 600 ev. Above this value the rate of increase of yield decreases and then becomes negative even though the total excitation of electrons within the crystal continues to increase. This indicates that above this primary energy significant numbers of low-energy electrons of the crystal are excited at depths too great for escape.

index directions for the two crystal orientations employed in Figs. 6 and 7. The low-index directions agree reasonably closely with the positions of the observed maxima.

A theoretical model to account for this phenomena has been proposed by Dekker[9] in which the primary electron beam is considered to be diffracted by a thin layer of the crystal at the surface of the target. The thickness of the diffracting region, which may be only a few atomic layers, corresponds to the path length within the crystal for which the primary electron wave retains coherence. Since the thickness of the diffracting layer is small, the diffraction which occurs is relatively insensitive to the primary electron energy.[9] The diffraction becomes most pronounced when the primary beam is directed parallel to a low-index crystalline direction. As a result of the diffraction, the primary electrons excite secondaries in regions closer to the crystal surface than would be the case if no diffraction occurred and the yield is consequently increased.

If the path length in which the primary electron wave retains coherence is large, as would be the case at high primary energies, the foregoing model involves diffraction from an extended three-dimensional lattice. Under this condition the diffraction phenomena are very sensitive to the energy of the primary electrons, diffraction occurring only for stringently specified angles and electron wavelengths. As a result the observed maxima would be expected to wash out at high primary energies,[9] an effect which has not been observed on MgO.

Another type of diffraction that does not wash out at high primary energies can be introduced as the basis of a model to account for the observed maxima. If a plane electron wave incident on a three-dimensional lattice undergoes an inelastic collision with an atom, the wave becomes localized and a new wave radiates from that point. Since this spherical wave may be strongly peaked in the direction of the incident plane wave but not coherent with it, the radiated wave may traverse a linear array of atoms giving rise to electron diffraction.[10] If the linear array corresponds to a low-index crystalline direction (small atomic spacing) the diffraction angles are large and, as in the previous model, enhancement of the yield may result.

Qualitatively these two models offer mechanisms which seem capable of accounting for some of the features of the maxima observed in the curve of yield vs angle of incidence, namely the angular positions of the maxima, the independence of the angle on the primary energy, and the broadness of the maxima. Detailed calculations are necessary to determine the validity of the models. Unfortunately, these models involve approximations ordinarily employed in electron diffraction work which may not be applicable here. In particular, the relations between the direction of the primary beam, lattice constants, angle of diffraction, and intensity of the diffracted beams are normally obtained by summing the scattered waves at points remote from the diffracting source. In the present problem the points at which such a summation should be made are limited by the path length in which the scattered waves retain coherence. Since this is the same order of magnitude as the thickness of the diffracting layer, the criterion of summing the scattered waves at a point remote from the scattering source is not fulfilled. Consequently, the validity of these models is open to question. In any case, the models do suggest that the observed maxima may be due to the scattering process from an orderly crystal structure and point out the importance of scattering in the secondary electron emission process.

V. CONCLUSIONS

The experiments reported here have demonstrated qualitatively the influence of the angle of incidence of the primary electron beam on the low-energy secondary electron spectra. The spectra exhibit relatively more low-energy electrons at normal incidence than at higher incidence angles in agreement with expectations.

The gross dependence of the total yield on the angle of incidence for MgO agrees qualitatively with descriptions relating yield and angle of incidence. A type of fine structure occurring as a series of maxima and minima superposed on the gross variation of yield with angle of incidence has been observed. The angular positions at which the maxima occur depend on the crystal orientation and are independent of the primary electron energy.

ACKNOWLEDGMENTS

The authors are indebted to a number of people for many discussions with regard to this work. In particular, thanks are due to V. L. Stout, J. R. Young, P. E. Pashler, and Professor W. G. Shepherd for their comments and suggestions, and to C. R. Bunting for assistance in making many of the measurements.

[9] A. J. Dekker, Phys. Rev. Letters **4**, 55 (1960).
[10] A. G. Emslie, Phys. Rev. **45**, 43 (1934); J. R. Tillman, Phil. Mag. **19**, 485 (1935).